Proceedings of 20th International Congress on Acoustics, ICA 2010

23-27 August 2010, Sydney, Australia

Dynamic Force Transmitted by a Nonlinear Hydraulic Engine Mount

Rajendra Singh* and Jong-Yun Yoon

Acoustics and Dynamics Laboratory, Smart Vehicle Concepts Center

The Ohio State University, Columbus, Ohio 43210 USA

PACS: 43.40. At, 43.40. Tm

ABSTRACT

Direct measurement of forces (with conventional force transducers) is not practical in many real-life applications since the interfacial conditions may change. Thus indirect force estimation methods must be developed, say by using other measured signals such as operating motions or pressures; however, applicable system properties must be known a priori. The indirect force estimation methods also pose special difficulty for hydraulic engine mounts that exhibit spectrally-varying and amplitude-sensitive parameters. This paper proposes new or refined procedures that will overcome some of the obstacles and thus provide a better estimate of the interfacial forces in the nonlinear hydraulic engine mount. First, the experimental time domain data from the non-resonant dynamic stiffness test is investigated for fixed and free decoupler designs. The fundamental and super-harmonic terms in the measured force and upper chamber pressure data are compared in the frequency domain up to 50 Hz. Second, mechanical and fluid models for fixed and free decoupler mounts are employed to relate motion and upper chamber pressure to the force transmitted by using a dual transfer path approach that is based on linear time-invariant system assumption. Third, the spectrally-varying and amplitude-sensitive parameters are determined by using the transfer functions from fluid models and steady state measurements. Fourth, the dynamic force is estimated by using alternate methods that employ measured excitation motion and/or upper chamber pressure signals. To include the nonlinear effect, the effective parameters for the quasi-linear model are defined only at the fundamental harmonic. Finally, the Fourier series expansions, with embedded transfer functions in terms of force to pressure (and force to motion), are utilized to calculate the precise forces transmitted to a rigid base. The proposed procedure shows that a quasi-linear model successfully predicts the dynamic forces transmitted by the nonlinear hydraulic mount in both time and frequency domains. Ongoing and future work will be briefly mentioned in the paper.

INTRODUCTION

Precise estimation of dynamic forces transmitted by a hydraulic engine mount is critical in designing machines, vehicle and buildings. Direct measurement of forces (for example, using conventional force transducers) is, however, not practical in many real-life applications since the interfacial conditions may change. Thus indirect force estimation methods must be developed. For instance, one could employ transfer path approaches, though they are applicable primarily in the frequency domain for a linear time-invariant system [1-3]. Also, dynamic forces could be estimated by using other measured signals such as operating motions, but then dynamic stiffness must be known a priori. Such indirect force estimation methods pose special difficulty for hydraulic engine mounts that exhibit spectrally-varying and amplitude-sensitive parameters. This article will propose new or refined methods to improve the dynamic force estimation method.

The dynamic characteristics of hydraulic engine mounts and its inherent nonlinear models have been examined and reported [4-13]. For instance, Singh et al. [4] studied the linear characteristics of both fixed and free decoupler mounts in low and high frequencies. Colgate et al. [5] employed equivalent linear models to examine the dynamic characteristics of hydraulic mount. Kim and Singh [6-7] showed the nonlinear models of chamber compliances and fluid resistances. Tiwari et al. [8] defined the curve-fit equations of nonlinear characteristics from inertia track resistances and upper and lower chamber compliances under the static preloads. He and Singh [9] examined the feasibility of analogous mechanical system models to expect the dynamic force transmitted to the rigid base in both time and frequency domains. Shangguan and Lu [10] examined the effect of temperature on fluid viscosity. Fan and Lu [11] investigated a function of plate inside the hydraulic mount experimentally. Lee and Singh [12-13] have studied the existence of super-harmonics in the hydraulic mount responses and the nonlinear behavior of a vehicle system. Main goal of this article is to improve the indirect force estimation method using excitation motion and/or upper chamber pressure with alternate transfer function methods.

PROBLEM FORMULATION

Figure 1 illustrates the experimental setup and schematic of hydraulic mount based upon the context of non-resonant dynamic stiffness testing procedure under the ISO standard 10846 [14]. Figure 2 describes the fluid model and its parameters by considering two force paths such as rubber and

hydraulic paths. Here, f_m is the preload; $x(t) = x_m + Re\left[\widetilde{X}e^{i\omega_o t}\right]$ is the excitation displacement; x_m is the mean displacement; $\widetilde{X} = Xe^{i\varphi_X}$; X is the excitation amplitude (zero-to-peak value); φ_X is the phase of $x(t)$, ω_o is the fundamental excitation frequency (rad/s); $Re[]$ is the real value operator; tilde over a symbol indicates the complex value. As measured data, the dynamic force transmitted to the rigid base is given from the force transducer. Also, the upper chamber pressuer $p_u(t)$ is measured using the pressure transduer installed in the upper chamber in our lab test. Based upon the given schematic shown in Figure 2, both rubber and hydraulic path forces can be calculated as follows in time (t) and frequency (ω) domains.

$$f_T(t) = f_{Tr}(t) + f_{Th}(t), \quad (1a)$$

$$f_{Tr}(t) = c_r\dot{x}(t) + k_r x(t), \; f_{Th}(t) = A_r p_u(t). \quad (1b,c)$$

$$\widetilde{F}_T(\omega) = \widetilde{F}_{Tr}(\omega) + \widetilde{F}_{Th}(\omega), \quad (2a)$$

$$\widetilde{F}_{Tr}(\omega) = \left(i\omega c_r + k_r\right)\widetilde{X}(\omega), \; \widetilde{F}_{Th}(\omega) = A_r\widetilde{P}_u(\omega). \quad (2b,c)$$

Here, $f_{Tr}(t)$ is the rubber path force (subscript r), $f_{Th}(t)$ is the hydraulic path force (subscript h), k_r and c_r are the rubber stiffness and damping coefficient respectively, A_r is the effective piston area, and $p_u(t)$ is the upper chamber pressure. As initial results, we can estimate the force transmitted to the rigid base by simply employing the given Eqns. (1a-c) and (2a-c) which is designated as a simple prediction model. The employed nominal parameters are as: $k_r = 2\times10^5$ *N/m*; $c_r = 496.1$ *N-s/m*; $A_r = 4\times10^{-3}$ m^2. Figure 3(a) compares the sinusoidal excitation displacement as an input displacement signal and the uppear chamber pressure as a response signal. Figure 3(b) shows the comparison between the measured and predicted force transmitted to the ridig base. As observed in Figures 3(a) and (b), the system shows the super-harmonic term in $f_T(t)$ and $p_u(t)$ even though the system is excited by the sinusoidal displacement $x(t)$. Also, the simple prediction model shows descripencies compared with the measured. Specifically the peak-to-peak values of the simple prediction model do not match well with the measured data even though the estimation with this model follows the same tendendy. Figure 4 shows the comparisions between measured and predicted transmitted forces in frequency domain. To estimate the force transmitted to the rigid base, Eqns. (2a-c) are used. As compared in Figure 4, the simple prediction model has big descripencies from the measured data. Thus, we need to improve the method to estimate the force transmitted to the rigid base by employing the effective parameters and alternate transferfunction methods. This will be announced in the later sections by employing quasi-linear models.

Our study will investigate the estimation of dynamic force transmitted to the rigid base with both fixed and free decoupler hydraulic mounts alone. The empolyied models are based on the fluid and analogous mechanical system models. The experiment and estimation will be considered up to 50 Hz over a range of X from 0.15 to 1.5 mm (zero-to-peak) under the steady state excitation condition. The specific objectives of this article are as follows: (1) Examine both rubber and hydraulic path forces in time and frequency domains. In order to estimate both path forces, the linear system transfer function that relates $\widetilde{F}_T$ to $\widetilde{X}$ (or $\widetilde{P}_u$) is determined; (2) the effective parameters in terms of the upper chamber compliance $\widetilde{C}_{ue}(\omega, X)$, rubber stiffness $k_{re}(\omega,X)$ and rubber damping $c_{re}(\omega,X)$ are investigated in both frequency and time domains. These effective parameters will be embedded in alternate transfer functions; (3) estimate force $f_T(t)$ in time domain by using the quasi-linear model and the Fourier expansion method incluing the fundamental ω_o.

LINEAR SYSTEM ANALYSIS WITH FLUID SYSTEM MODEL

A lumped model of the fluid system illustrated in Figure 2 could be considered with the followsing assumptions: (1) the given system is a linear time-invariatn system with nominal fluid system parameters; (2) the mount is bound to the rigid base and excited by the steady state sinusoidal displacement $x(t)$; (3) the force transmitted to the rigid base consists of both rubber and hydraulic force paths. Based upon the described assumptions, the momentum and continuity equations can be derived as follows. The detailed derivation could be referred to the literatures [4, 6-9].

$$p_u(t) - p_l(t) = I_i\dot{q}_i(t) + R_i q_i(t), \quad (3b)$$

$$p_u(t) - p_l(t) = I_d\dot{q}_d(t) + R_d q_d(t), \quad (3c)$$

$$C_u\dot{p}_u(t) = A_r\dot{x}(t) - q_i(t) - q_d(t), \quad (3d)$$

$$C_l\dot{p}_l(t) = q_i(t) + q_d(t). \quad (3e)$$

Here, C_u and C_l are the upper (#*u*) and lower (#*l*) chamber compliances respectively; I_i and I_d are the inertances of the inertia track and decoupler respectively; R_i and R_d are the resistances of the inertia track and decoupler respectively; and q_i and q_d are the fluid flow through intertia track and decoupler respectively. Transform Eqns. (1a-c) and (3a-e) into the Laplace domain (s) by assuming that the initial conditions are zeros.

$$F_T(s) = \left(c_r s + k_r\right)X(s) + A_r P_u(s), \quad (4a)$$

$$F_T(s) = F_{Tr}(s) + F_{Th}(s), \quad (4b)$$

$$F_{Tr}(s) = \left(c_r s + k_r\right)X(s), \; F_{Th}(s) = A_r P_u(s), \quad (4c,d)$$

$$P_u(s) - P_l(s) = \left(I_i s + R_i\right)Q_i(s), \quad (4e)$$

$$P_u(s) - P_l(s) = \left(I_d s + R_d\right)Q_d(s), \quad (4f)$$

$$C_u sP_u(s) = A_r sX(s) - Q_i(s) - Q_d(s), \quad (4g)$$

$$C_l sP_l(s) = Q_i(s) + Q_d(s). \quad (4h)$$

Now we can develop the relationships of $F_T(s)$ to $X(s)$ and $F_T(s)$ to $P_u(s)$ further. First, the relationship between $P_u(s)$ and $X(s)$ can be derived with respect to the fixed decoupler mount by assuming that $I_d = 0$ and $R_d \to \infty$:

$$\frac{P_u}{X}(s) = \frac{A_r\left(C_l I_i s^2 + C_l R_i s + 1\right)}{C_u C_l I_i s^2 + C_u C_l R_i s + \left(C_u + C_l\right)} \quad (5)$$

Second, the free decoupler mount has the following formulation under the assumption that $I_d \approx 0$ below 50 Hz:

$$\frac{P_u}{X}(s) = \frac{A_r\left[C_l I_i R_d s^2 + \left(C_l R_i R_d + I_i\right)s + \left(R_i + R_d\right)\right]}{C_u C_l I_i R_d s^2 + \left[C_u C_l R_i R_d + \left(C_u + C_l\right)I_i\right]s + \left(C_u + C_l\right)\left(R_i + R_d\right)} \quad (6)$$

From the given Eqns. (5) and (6), the standard formulation designated as the dimensionless pressure to displacement transfer function $\overline{G}(s)$ can be derived with some dimensionless variables and parameters: $\overline{X} = X/X_{ref}$ = the dimensionless excitation displacement amplitude; X_{ref} = reference displacement amplitude; $\overline{P}_u = P_u/P_{uref}$ = dimensionless pressure; $P_{uref} = (k_{rref}\, X_{ref})/A_r$ = reference

pressure; k_{rref} = reference stiffness; $\overline{F}_T = F_T/F_{Tref}$ = dimensionless force; and $F_{Tref} = k_{rref}X_{ref}$ = reference force.

$$\overline{G}(s) = \frac{\overline{P_u}}{\overline{X}}(s) = \frac{A_r}{k_{rref}}\frac{P_u}{X}(s)$$

$$= \gamma_h\left(\frac{s^2}{\omega_{N1}^2} + \frac{2\zeta_1}{\omega_{N1}}s + 1\right) / \left(\frac{s^2}{\omega_{N2}^2} + \frac{2\zeta_2}{\omega_{N2}}s + 1\right), \quad (7a)$$

$$\gamma_h = \frac{A_r^2}{k_{rref}\left(C_u + C_l\right)},\ \zeta_{1(fixed)} = \frac{1}{2}\sqrt{\frac{C_l R_i^2}{I_i}}, \quad (7b,c)$$

$$\zeta_{1(free)} = \frac{1}{2}\left(\sqrt{\frac{C_l R_d R_i^2}{I_i\left(R_i + R_d\right)}} + \sqrt{\frac{I_i}{C_l R_d\left(R_i + R_d\right)}}\right), \quad (7d)$$

$$\zeta_{2(fixed)} = \frac{1}{2}\sqrt{\frac{C_u C_l R_i^2}{I_i\left(C_u + C_l\right)}}, \quad (7e)$$

$$\zeta_{2(free)} = \frac{1}{2}\left[\sqrt{\frac{C_u C_l R_d R_i^2}{I_i\left(C_u + C_l\right)\left(R_i + R_d\right)}} + \sqrt{\frac{\left(C_u + C_l\right)I_i}{C_u C_l R_d\left(R_i + R_d\right)}}\right], \quad (7f)$$

$$\omega_{N1(fixed)} = \sqrt{\frac{1}{C_l I_i}},\ \omega_{N1(free)} = \sqrt{\frac{R_i + R_d}{C_l I_i R_d}} \quad (7g,h)$$

$$\omega_{N2(fixed)} = \sqrt{\frac{C_u + C_l}{C_u C_l I_i}}, \quad (7i)$$

$$\omega_{N2(free)} = \sqrt{\frac{\left(C_u + C_l\right)\left(R_i + R_d\right)}{C_u C_l I_i R_d}}. \quad (7j)$$

Here, the transfer function is expressed in terms of natural frequencies (ω_{N1} and ω_{N2}), damping ratios (ζ_1 and ζ_2) and hydraulic path static stiffness γ_h, and their expressions are described in Eqns. (7a-j). Subscripts (fixed) and (free) are designated as the system parameters for the fixed and free decouplers respectively. From the relationships between Eqns. (4a-d) and (7a-j), the dimensionless dynamic stiffness $\overline{K}(s)$ and its rubber $\overline{K}_r(s)$ and hydraulic $\overline{K}_h(s)$ components are described as follows:

$$\overline{K}(s) = \overline{K}_r(s) + \overline{K}_h(s), \quad (8a)$$

$$\overline{K}_r(s) = \frac{\overline{F}_{Tr}}{\overline{X}}(s) = \gamma_r\left(1 + \tau_r s\right), \quad (8b)$$

$$\overline{K}_h(s) = \frac{\overline{F}_{Th}}{\overline{X}}(s)$$

$$= \gamma_h\left(\frac{s^2}{\omega_{N1}^2} + \frac{2\zeta_1}{\omega_{N1}}s + 1\right) / \left(\frac{s^2}{\omega_{N2}^2} + \frac{2\zeta_2}{\omega_{N2}}s + 1\right), \quad (8c)$$

$$\tau_r = \frac{c_r}{k_r},\ \gamma_r = \frac{k_r}{k_{rref}}. \quad (8d,e)$$

Here, τ_r and γ_r are the time constant and static stiffness of the rubber path modeled using the Voight model. Also, the dimensionless dynamic force transmissibility $\overline{H}(s)$ is derived with its rubber $\overline{H}_r(s)$ and hydraulic $\overline{H}_h(s)$ components using Eqns. (7a-j) and (8a-e) as follows:

$$\overline{H}(s) = \overline{H}_r(s) + \overline{H}_h(s), \quad (9a)$$

$$\overline{H}_r(s) = \frac{\overline{F}_{Tr}}{\overline{P}_u}(s)$$

$$= \frac{\gamma_r}{\gamma_h}\left(1 + \tau_r s\right)\left(\frac{s^2}{\omega_{N2}^2} + \frac{2\zeta_2}{\omega_{N2}}s + 1\right) / \left(\frac{s^2}{\omega_{N1}^2} + \frac{2\zeta_1}{\omega_{N1}}s + 1\right), \quad (9b)$$

$$\overline{H}_h(s) = \frac{\overline{F}_{Th}}{\overline{P}_u}(s) = 1. \quad (9c)$$

In this article, the employed nominal parameters are as follows: I_i = 4×10^6 kg/m^4; I_d = 509.3 kg/m^4; C_u = 2.5×10^{-11} m^5/N; C_l = 2.4×10^{-9} m^5/N; R_i = 2×10^8 N-s/m^5; R_d = 5×10^8 N-s/m^5; A_r = 4.5×10^{-3} m^2. Reference values are selected as: k_{rref} = 2.0×10^5 N/m; and X_{ref} (×10^{-3} m) though different values of X_{ref} according to the experimental excitation amplitudes are utilized.

LINEAR SYSTEM ANALYSIS WITH ANALOGOUS MECHANICAL SYSTEM MODEL

Figure 5 illustrates the analogous mechanical system model based upon the linear time-invariant system with effective mechanical parameters from the fluid system properties. The basic equations are derived as follows:

$$m_{ie}\ddot{x}_{ie}(t) + c_{ie}\dot{x}_{ie}(t) + \left(k_u + k_l\right)x_{ie}(t) = k_u x(t) \quad (10)$$

$$f_T(t) = c_r\dot{x}(t) + k_r x(t) + k_l x_{ie}(t) \quad (11)$$

Here, the employed mechanical parameters are defined as follows: effective mass of inertia track fluid column $m_{ie} = A_r^2 I_i$; effective viscous damping of inertia track fluid $c_{ie} = A_r^2 R_i$; equivalent stiffness of upper chamber compliance $k_u = A_r^2/C_u$; equivalent stiffness of lower chamber compliance $k_l = A_r^2/C_l$; and effective velocity of inertia track fluid $\dot{x}_{ie}(t) = q_i(t)/A_r$. By transforming Eqns. (10) and (11) into the Laplace domain (s) with the initial conditions equal to zero, the dimensionless transfer functions are expressed as follows:

$$\overline{K}_A(s) = \overline{K}_{Ar}(s) + \overline{K}_{Ah}(s), \quad (12a)$$

$$\overline{K}_{Ar}(s) = \frac{\overline{F}_{Ar}}{\overline{X}}(s) = \gamma_r\left(1 + \tau_r s\right), \quad (12b)$$

$$\overline{K}_{Ah}(s) = \frac{\overline{F}_{Ah}}{\overline{X}}(s) = \gamma_h \Big/ \left(\frac{s^2}{\omega_{N2}^2} + \frac{2\zeta_2}{\omega_{N2}}s + 1\right). \quad (12c)$$

Here, $\overline{K}_A(s)$ is the dimensionless dynamic stiffenss (subscript A) of the analogous mechanical system, $\overline{K}_{Ar}(s)$ and $\overline{K}_{Ah}(s)$ are the rubber and hydraulic path forces repectively. The employed nominal parameters are: m_{ie} = 81 kg; c_{ie} = 4.1×10^3 N-s/m; k_u = 8.1×10^5 N/m; k_l = 8.4×10^3 N/m. Thus, our study will focus on the fluid system models as described in Eqns. (8a-e) and (9a-c), and the analogous mechanical system model in Eqns. (12a-c).

SPECTRALLY-VARYING AND AMPLITUDE-SENSITIVE PROPERTIES

Effective hydraulic force path parameter at fundamental harmonic

The effective upper chamber compliance $\widetilde{C}_{ue}(\omega, X)$ can be calculated at fundamental ω_o. To find out the $\widetilde{C}_{ue}(\omega, X)$, the hydraulic path force path parameter $\widetilde{\lambda}_u(\omega, X)$ is considered using the measured data in terms of upper chamber pressure $\widetilde{P}_{uM}(\omega, X)$ and the excitation displacement $\widetilde{X}_M(\omega)$.

First, $\widetilde{C}_{ue}(\omega, X)$ can be considered as follows:

$$\widetilde{C}_{ue}(\omega,X) = C_{u\mathbf{n}}\,\widetilde{\lambda}_u(\omega,X), \quad (13a)$$

$$\widetilde{\lambda}_u(\omega,X) = (\alpha + i\beta). \quad (13b)$$

Here, $C_{u\mathbf{n}}$ is the nominal value of upper chamber compliance. The complex valued term $\widetilde{P}_{uM}(\omega,X)$ is expressed as follows by replacing *s* with $i\omega$ in the frequency domain with fundamental harmonic term from the given Eqn. (5) for the fixed decoupler:

$$\widetilde{P}_u(\omega,X) = \frac{A_r\left[\left(1-\omega^2 C_l I_i\right) + i\omega C_l R_i\right]X}{\left(C_u + C_l - \omega^2 C_u C_l I_i\right) + i\omega C_u C_l R_i} \quad (14)$$

From Eqns. (13a,b) and (14), $\widetilde{\lambda}_u(\omega,X)$ is estimated by two terms α and β with a function of ω and *X*. In order to calculate α and β, the measured $\widetilde{P}_{uM}(\omega,X)$ is considered as a complex values given by measured magnitude $\left|\widetilde{P}_{uM}\right|$ and phase ϕ_M as below:

$$\widetilde{P}_{uM} = P_{u\mathbf{RE}} + iP_{u\mathbf{IM}}, \quad (15a)$$

$$P_{u\mathbf{RE}} = Re\left[\widetilde{P}_{uM}\right] = \left|\widetilde{P}_{uM}\right| cos(\phi_M), \quad (15b)$$

$$P_{u\mathbf{IM}} = Im\left[\widetilde{P}_{uM}\right] = \left|\widetilde{P}_{uM}\right| sin(\phi_M). \quad (15c)$$

Here, the subscript ***RE*** and ***IM*** are designated as the real and imaginary number repectively. The estimation of $\widetilde{\lambda}_u(\omega,X)$ with respect to the fundamental and super-harmnoc terms is referred to the literatures [15, 16].

Effective rubber force path parameter

The linear system analysis in the previous sections has suggested both rubber and hydraulic force paths, and thus, we need to examine the dynamic rubber path properties with the same manner investigated for $\widetilde{C}_{ue}(\omega,X)$. Figure 6 shows the one data set with *X* = 0.15 mm with respect to the rubber stiffness and damping properties. The test is done when fluid is drained from the same hydraulic mount. As shown in Figure 6, rubber path force is also affected from the rubber path properties spectrally corresponding to different excitation displcement *X*. The effective stiffness $k_{re}(\omega,X)$ can be estimated as $k_{r\mathbf{n}}\,\lambda_{kr}(\omega,X)$, and $c_{re}(\omega,X)$ as $c_{r\mathbf{n}}\,\lambda_{cr}(\omega,X)$ where $k_{r\mathbf{n}}$ and $c_{r\mathbf{n}}$ are the nominal (linear system) values of k_r and c_r respectively. $\lambda_{kr}(\omega,X)$ and $\lambda_{cr}(\omega,X)$ are spectrally-varying and amplitude-sensitive parameters for k_r and c_r, respectively [15,16]. Thus, by including the effective properties from the rubber force path, the combined effective forces from elastomeric and hydraulic parts within the mount will improve the dynamic force estimation. The methods to estimate the continuous curve-fit schemes of $\lambda_{kr}(\omega,X)$ and $\lambda_{cr}(\omega,X)$ can be referred to the literatures [15,16].

DYNAMIC FORCE ESTIMATION USING QUASI-LINEAR MODELS

Alternate transfer function schemes

Alternate transfer function schemes could be considered based on Eqns. (4a), (8a-e), (9a-c), and (12a-c) along with quasi-linear models designated as Schemes *I, II, III* and *IV* respectively. Thus, the steady state responses are examined by changing the *s* term to $i\omega$ with each scheme. These are listed in Table 1. Table 1 describes alternate schemes with the relevant measured data such as $\widetilde{X}(\omega)$ and/or $\widetilde{P}_u(\omega,X)$. Scheme *I* is the simplest estimation of $\overline{F}_T(\omega,X)$ with Eqn. (4a), Scheme *II* shows the force estimation from the dynamic stiffness by the relationship of $\overline{F}_T(\omega,X)$ to *X*, Scheme *III* illustrates the direct relationship of $\overline{F}_T(\omega,X)$ to $\overline{P}_u(\omega,X)$ and Scheme *IV* is the analogous mechanical system model. The suggested schemes can incorporate spectrally-varying and amplitude-sensitive parameters $\lambda_v(\omega,X)$ (*v* = *u, kr, cr*) under the sinusoidal excitation with amplitude *X*. If the scheme has the parameter $\lambda_v(\omega,X)$ = 1 (*v* = *u, kr, cr*), $\overline{F}_T(\omega,X)$ is estimated by the linear model with only nominal values. Thus, the proposed schemes (*I, II, III* and *IV*) are devided into *A, B* and *C* such as *II-A, II-B* and *II-C*. Also, the merits of each method could be considered with repect to the number of sensors needed and main concerns in terms of the transfer functions such as $\overline{K}(s)$ or $\overline{H}(s)$.

Table 1. Comparison of alternate force estimation schemes based on quasi-linear model

Scheme Designation		Sensor(s) required		Spectrally-varying and amplitude-sensitive parameters
		X	P_u	
Fluid System Model (Figure. 2)	*I-A*	Yes	Yes	$\lambda_{kr}=1,\ \lambda_{cr}=1$
	I-B	Yes	Yes	$\lambda_{kr}\neq 1,\ \lambda_{cr}\neq 1$
	II-A	Yes	No	$\lambda_{kr}=1,\ \lambda_{cr}=1,\lambda_u\neq 1$
	II-B	Yes	No	$\lambda_{kr}\neq 1,\ \lambda_{cr}\neq 1,\lambda_u=1$
	II-C	Yes	No	$\lambda_{kr}\neq 1,\ \lambda_{cr}\neq 1,\lambda_u\neq 1$
	III-A	No	Yes	$\lambda_{kr}=1,\ \lambda_{cr}=1,\lambda_u\neq 1$
	III-B	No	Yes	$\lambda_{kr}\neq 1,\ \lambda_{cr}\neq 1,\lambda_u=1$
	III-C	No	Yes	$\lambda_{kr}\neq 1,\ \lambda_{cr}\neq 1,\lambda_u\neq 1$
Analogous Mechanical System Model (Figure. 5)	*IV-A*	Yes	No	$\lambda_{kr}=1,\ \lambda_{cr}=1,\lambda_u\neq 1$
	IV-B	Yes	No	$\lambda_{kr}\neq 1,\ \lambda_{cr}\neq 1,\lambda_u=1$
	IV-C	Yes	No	$\lambda_{kr}\neq 1,\ \lambda_{cr}\neq 1,\lambda_u\neq 1$

Force estimation with quasi-linear (*QL*) models in time domain

The Fourier series expansion is employed for the relevant schemes in order to estimate $f_T(t)$ using a transfer function $\overline{K}_e$ or $\overline{H}_e$ embeding k_{re}, c_{re} and $\widetilde{C}_{ue}$ as described in Table 1. In order to estimate the dynamic force transmitted to the rigid base, the mount is assumed to be excited under steady state condition. Thus, the input displacement *x(t)* is defined as $Re\left[\widetilde{X}e^{i\omega_o t}\right] = Re\left[Xe^{i(\omega_o t+\varphi_X)}\right]$ where *X* and φ_X are the amplitude and phase. The dynamic force is estimated as described below where the dynamic stiffness $\overline{K}_e(\omega_o,X)$ and force transmissibility $\overline{H}_e(\omega_o,X)$ are the formulations embedded by k_{re}, c_{re} and $\widetilde{C}_{ue}$ at fundamental ω_o:

$$f_{T-SchemeII}(t) = f_m + \chi_1\left|\overline{K}_e(\omega_o,X)\right| Re\left[e^{i(\omega_o t+\varphi_X+\varphi_{\overline{K}})}\right], \quad (16a)$$

$$\chi_1 = k_{rref}X_{ref}\overline{X},\ \varphi_{\overline{K}} = \angle\overline{K}_e(\omega_o,X). \quad (16b)$$

$$f_{T-SchemeIII}(t) = f_m + \chi_2\left|\overline{H}_e(\omega_o,X)\right| Re\left[e^{i(\omega_o t+\varphi_{\overline{P1}}+\varphi_{\overline{H}})}\right], \quad (17a)$$

$$\chi_2 = k_{rref}X_{ref}\left|\overline{P}_u(\omega_o,X)\right|, \quad (17b)$$

$$\varphi_{\overline{P1}} = \angle\overline{P}_u(\omega_o,X),\ \varphi_{\overline{P1}} = \angle\overline{H}_e(\omega_o,X). \quad (17c,d)$$

Here, the χ_1 and χ_2 terms are used for evaluating the $f_T(t)$ history in force units (N) from the normalized values. Also,

$f_{T\text{-}SchemeII}(t)$ and $f_{T\text{-}SchemeIII}(t)$ are the force estimations by the schemes *II-C* and *III-C* respectively.

RESULTS AND DISCUSSION

Figures 7 and 8 compare the results of both linear and quasi-linear models with experiment in frequency domain. The results shown in Figures 7 and 8 are the estimated dimensionless forces. Schemes *I* and *II* successfully predict the dynamic force transmitted to the rigid base for both fixed and free decouplers. Schemes *III* also shows good correlation except at X = 0.15 mm for the free decoupler. The linear model shows similar tendency of the dynamic force, but does not predict the precise magnitude and phase. Specifically the linear model in Figure 8 (a) reveals a significant deviation compared with the experiment. Scheme *IV* based on the analogous mechanical system model fails to predict the forces. All the magnitudes and phases of Scheme *IV* are almost constant as observed in Figures 7 and 8. The cause of deficiency from Scheme *IV* can be found out when Eqns. (8c) and (12c) are compared. The hydraulic force path as shown in Eqn. (12c) for Scheme *IV* does not have any effective mechanical properties on the numerator. Figure 9 compares the time histories as predicted by Eqns. (16a,b) and (17a-d) with measured forces for the free decoupler mount at f = 8.5 Hz and X = 1.5 mm. This result is a significant improvement over the previous formulation as illustrated in Figure 3. When the quasi-linear models for both rubber and hydraulic force paths are employed, the estimation of $f_T(t)$ matches well with measured force specifically in terms of its amplitude. The discrepancies between the experiment and the proposed models are primarily due to the super-harmonic terms, which are not included in the current study. A future article will address this issue further with focus on the super-harmonic responses [16].

CONCLUSION

This article has proposed new or refined dynamic force estimation methods by using alternate transfer function schemes that are embedded in quasi-linear models. Specific contributions of this article include the following. First, the super-harmonic contents of measured upper chamber pressure $p_{uM}(t)$ and force $f_{TM}(t)$ are examined and correlated up to 50 Hz from the non-resonant dynamic stiffness test. Second, alternate relevant transfer function formulations with fundamental ω_o terms are examined in both frequency and time domains. Also, the fluid and analogous mechanical system models are compared and examined based upon the linear time-invariant system assumption. Third, a quasi-linear model with amplitude-sensitive and spectrally-varying parameters such as $\widetilde{C}_{ue}(\omega, X)$, $k_{re}(\omega,X)$ and $c_{re}(\omega,X)$ has been investigated. By embedding these effective parameters into quasi-linear models, the effect of mount nonlinearities on the dynamic force transmitted to the rigid base is quatifined with rubber and hydraulic path forces. A more refined nonlinear model needs to be developed to successfully predict the super-harmonic responses; this issue is the focus of a future article [16]. Yet another article will examine the measurement of in situ dynamic forces [17].

ACKNOWLEDGEMENT

We are grateful to the member organizations of the Smart Vehicle Concepts Center (www.SmartVehicleCenter.org) and the National Science Foundation Industry/University Cooperative Research Centers program (www.nsf.gov/eng/iip/iucrc) for supporting this work.

REFERENCES

1 A. Inoue, R. Singh and G. A. Fernandes, "Absolute and relative path measures in a discrete system by using two analytical methods" *J. Sound Vib*. **313**, 696-722 (2008)
2 A. Gunduz, A. Inoue and R. Singh, "Estimation of interfacial forces in time domain for linear system" *J. Sound Vib.* **329**, 2616-2634 (2010)
3 Q. Leclere, C. Pezerat, B. Laulagnet and L. Polac, "Indirect measurement of main bearing loads in an operating diesel engine" *J. Sound Vib.* **286**, 341-361 (2005)
4 4 R. Singh, G. Kim and P.V. Ravindra, "Linear analysis of automotive hydro-mechanical mount with emphasis on decoupler characteristics" *J. Sound Vib*. **158**(2), 219-243 (1992)
5 J.E. Colgate, C.T. Chang, Y.C. Chiou, W.K. Liu and L.M. Keer, "Modeling of a hydraulic engine mount focusing on response to sinusoidal and composite excitations" *J. Sound Vib.* **184**(3), 503-528 (1995)
6 G. Kim and R. Singh, "Nonlinear analysis of automotive hydraulic engine mount" *ASME J. Dyn. Syst. Meas. Control* **115**(3), 482-487 (1993)
7 G. Kim and R. Singh, "A study of passive and adaptive hydraulic engine mount systems with emphasis on nonlinear characteristics" *J. Sound Vib.* **179**(3), 427-453 (1995)
8 M. Tiwari, H. Adiguna and R. Singh, "Experimental characterization of a nonlinear hydraulic engine mount" *Noise Control Eng. J.* **51**(1), 36-49 (2003)
9 S. He and R. Singh, "Estimation of amplitude and frequency dependent parameters of hydraulic engine mount given limited dynamic stiffness measurements" *Noise Control Eng. J.* **53**(6), 271-285 (2005)
10 W.B. Shangguan and Z.H. Lu, "Experimental study and simulation of a hydraulic engine mount with fully coupled fluid-structure interaction finite element analysis model" *Comput. Struct.* **82**, 1751-1771 (2004)
11 R. Fan and Z. Lu, "Fixed points on the nonlinear dynamic properties of hydraulic engine mounts and parameter identification method: Experiment and theory" *J. Sound Vib.* **305**, 703-727 (2007)
12 J.H. Lee and R. Singh, "Nonlinear frequency responses of quarter vehicle models with amplitude-sensitive engine mounts" *J. Sound Vib.* **313**, 784-805 (2003)
13 J.H. Lee and R. Singh, "Existence of super-harmonics in quarter-vehicle system responses with nonlinear inertia hydraulic track mount given sinusoidal force excitation" *J. Sound Vib.* **313**, 367-374 (2008)
14 Acoustics and vibration - Laboratory measurement of vibro-acoustic transfer properties of resilient elements *ISO 10846: 1997*, (International Organization for Standardization, Geneva, Switzerland, 1997)
15 J.Y. Yoon and R. Singh, "Dynamic force transmitted by hydraulic mount: Estimation in frequency domain using motion and/or pressure measurements and quasi-linear models" *accepted for publication in the Noise Control Engineering Journal*, (April 2010)
16 J.Y. Yoon and R. Singh, "Indirect measurement of dynamic force transmitted by a nonlinear hydraulic mount under sinusoidal excitation with focus on super-harmonics" *submitted to the Journal of Sound and Vibration*, (May 2010)
17 J.Y. Yoon and R. Singh, "Estimation of Interfacial Foces" *SVC project # 20 report (in progress)*, (2009-2010)

(a)

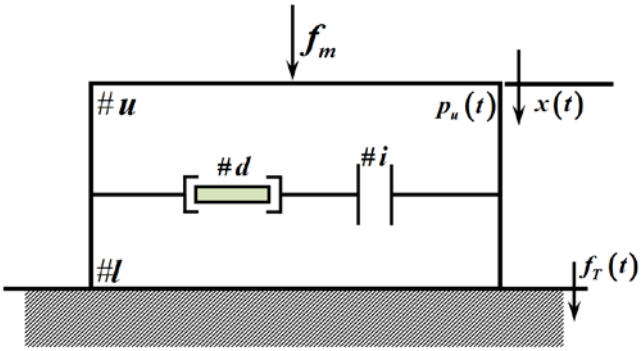

(b)

Figure 1. Force $f_T(t)$ transmitted by a hydraulic mount in the context of non-resonant elastomeric test [14]: (a) Experimental setup with a hydraulic mount; (b) Schematic of the hydraulic mount and measurements.

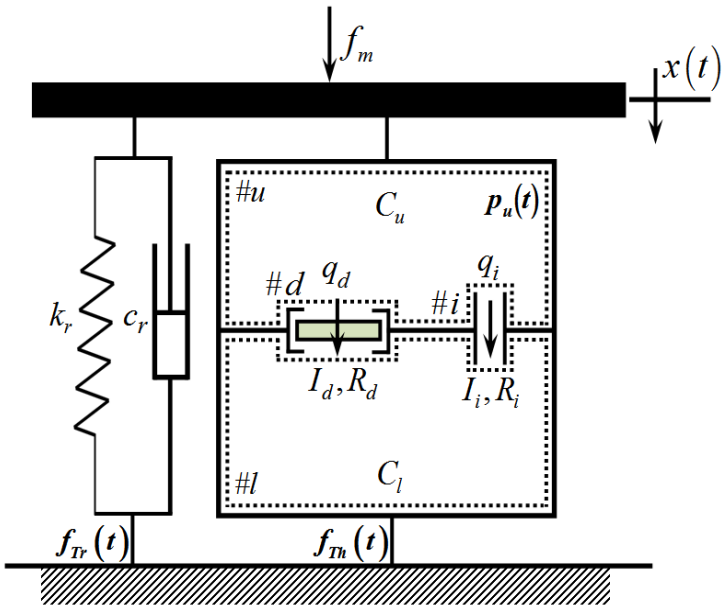

Figure 2. Fluid model of the hydraulic mount and its parameters with rubber and hydraulic paths.

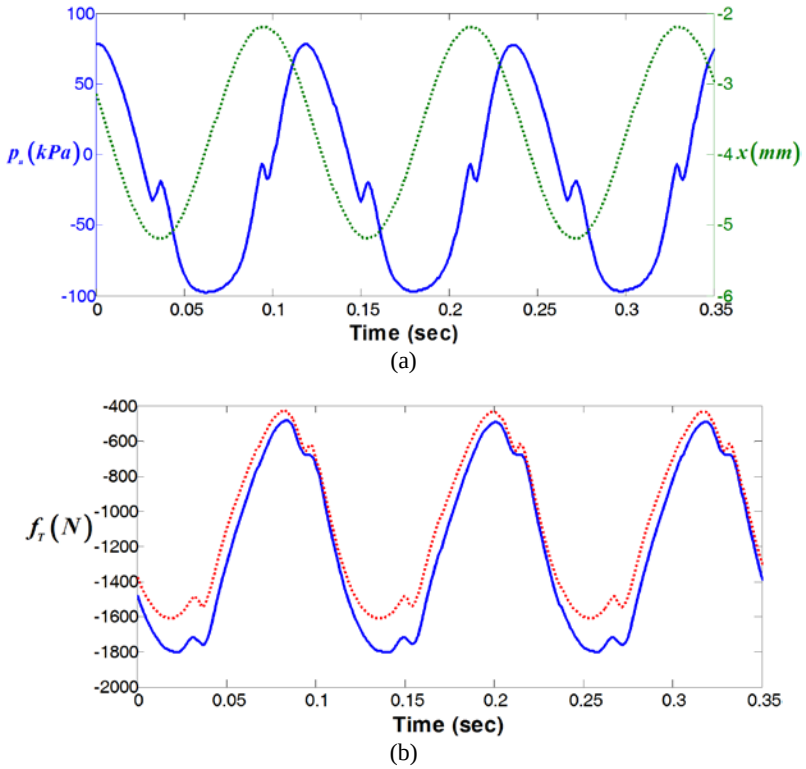

Figure 3. Comparison between measured and predicted transmitted force time histories for the free decoupler mount, given sinusoidal displacement $x(t) = x_m + Re\left[\widetilde{X}e^{i\omega_o t}\right]$ at $\omega_o/2\pi$ = 8.5 Hz and X = 1.5 mm: (a) measured $x(t)$ with X = 1.5 mm and $p_u(t)$ time histories; Key for part (a): ·····, $x(t)$; ——, $p_u(t)$; (b) measured and predicted force, $f_T(t)$; Key for part (b); ——, experiment; ·····, theory (Eqns. (1a-c) given nominal parameters).

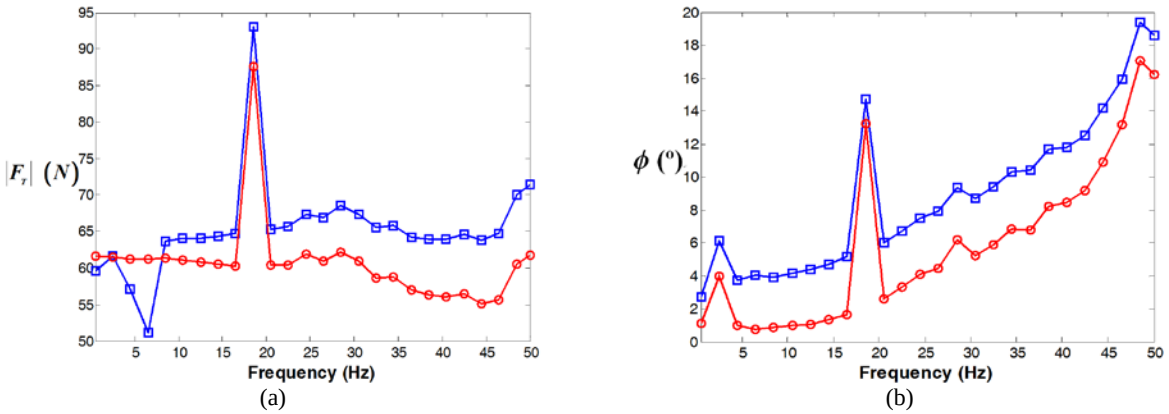

Figure 4. Comparison between measured and predicted transmitted forces, $\left|\widetilde{F}_T\left(\omega_o, X\right)\right|$ for the free decoupler mount given X = 0.15 mm: (a) magnitude spectra; (b) phase spectra. Key: ⊟, experiment; ⊖, theory (Eqns. (2a-c) given nominal parameters).

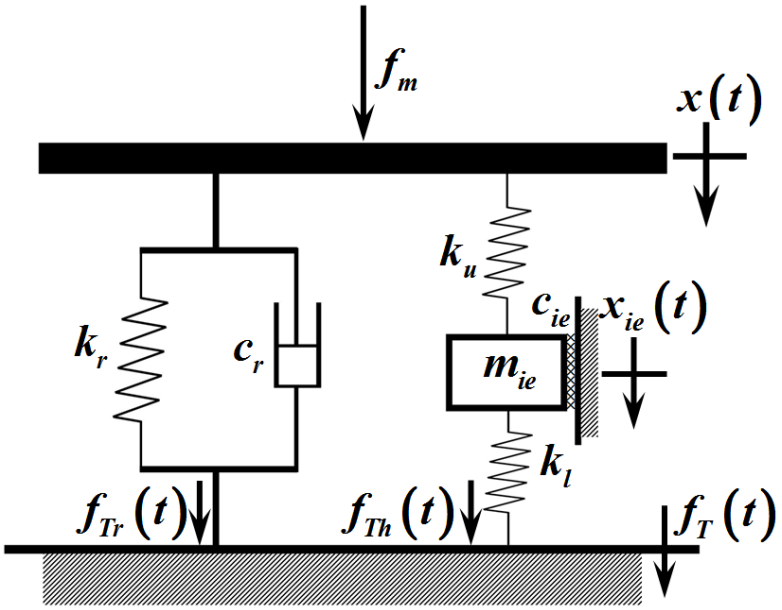

Figure 5. Analogous mechanical system model and its parameters for rubber and hydraulic paths.

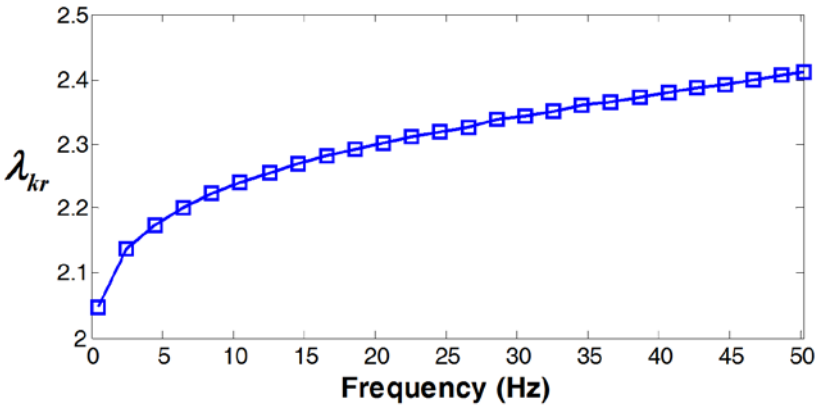

(a)

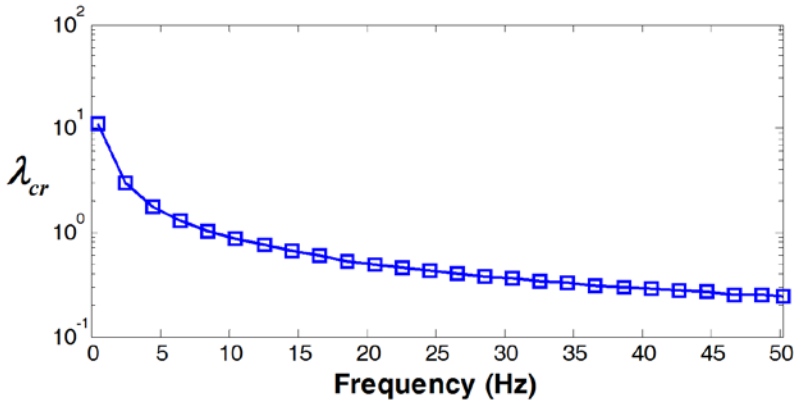

(b)

Figure 6. Spectrally-varying and amplitude-sensitive properties of the rubber path with X = 0.15 mm: (a) effective stiffness quantified by λ_{kr} $(=k_{re}/k_{rn})$ and displayed on a linear scale; (b) viscous damping quantified by λ_{cr} $(=c_{re}/c_{rn})$ and displayed on a $\log_e$ scale.

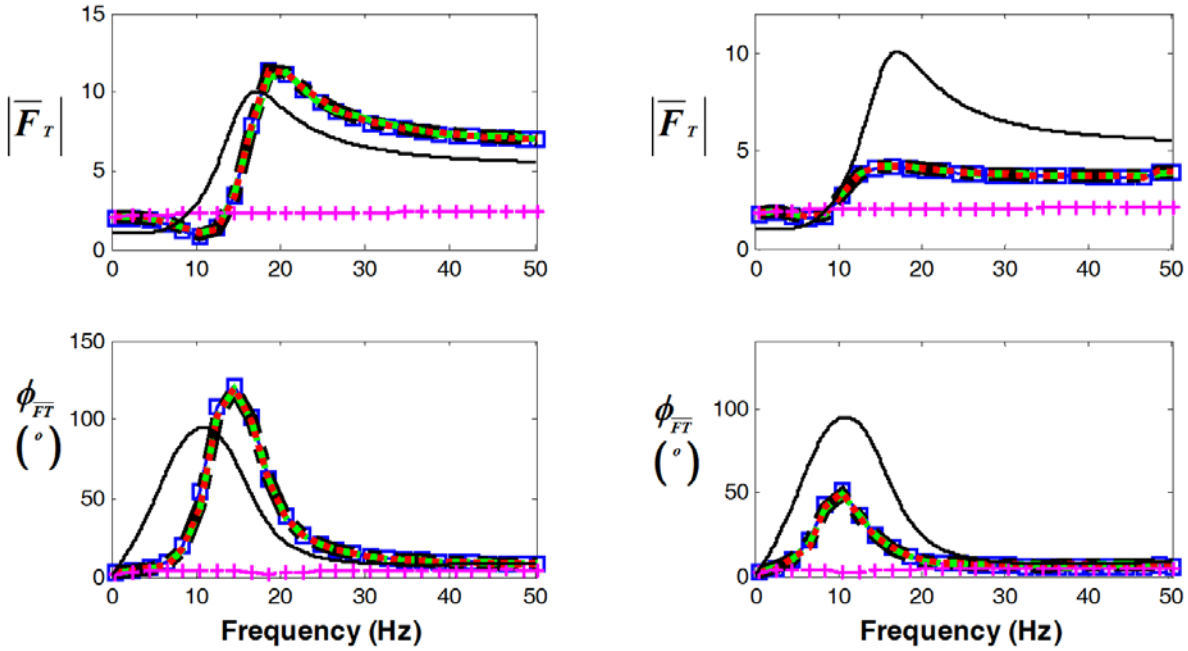

Figure 7. Force transmitted to the rigid base by a fixed decoupler mount: (a) X = 0.15 mm; (b) X = 1.5 mm. Key: ⊟, experiment; ——, linear model; – · , Scheme *I*; – – , Scheme *II*; ····, Scheme *III*; ⊣, Scheme *IV*.

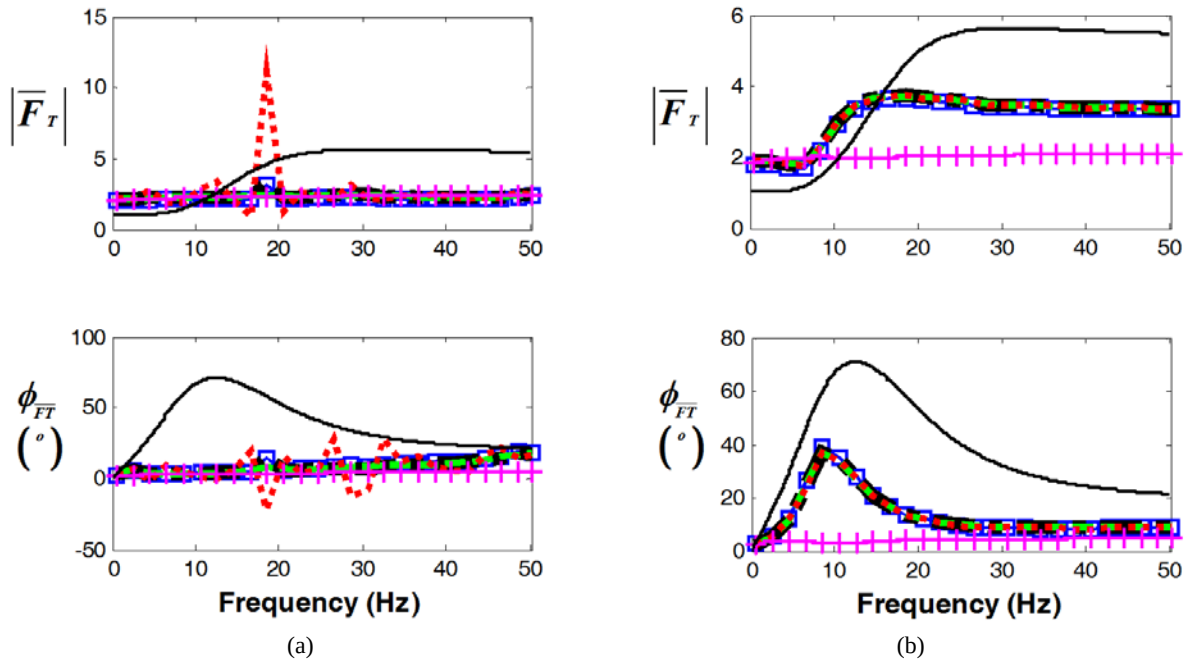

Figure 8. Force transmitted to the rigid base by a free decoupler mount: (a) X = 0.15 mm; (b) X = 1.5 mm. Key: ⊟, experiment; ——, linear model; – · , Scheme *I*; – – , Scheme *II*; ····, Scheme *III*; ⊣, Scheme *IV*.

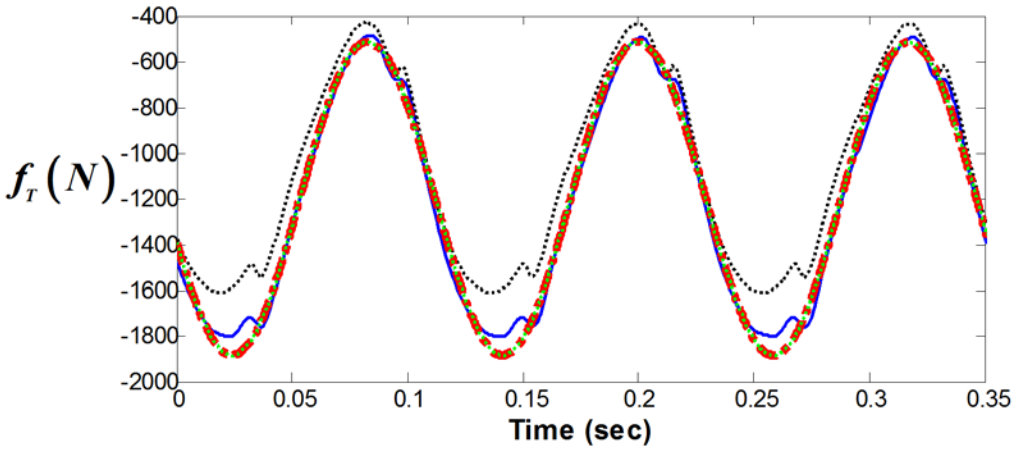

Figure 9. Comparison between measured and predicted forces in time domain for the free decoupler mount, given sinusoidal displacement $x(t) = x_m + Re\left[\widetilde{X}e^{i\omega_o t}\right]$ at $\omega/2\pi$ = 8.5 Hz and X = 1.5mm. Key: ——, experiment ; ·····, estimation by Eqns. (1a-c) given nominal parameters; — · , estimation by Scheme *II-C* with quasi-linear parameters; ····, estimation by Scheme *III-C* with quasi-linear parameters.